

**BJP**

**Bangladesh Journal of Pharmacology**

**Research Article**

**A PLK1 inhibitor, RO3280, suppresses proliferation of SNU-16 gastric cancer cells via apoptosis**

# A PLK1 inhibitor, RO3280, suppresses proliferation of SNU-16 gastric cancer cells via apoptosis

Fatih Yulak<sup>1</sup> and Zekeriya Keskin<sup>2</sup>

<sup>1</sup>Departments of Physiology, School of Medicine, Cumhuriyet University, Sivas, Turkey; <sup>2</sup>Department of Internal Medicine, Sivas Sarkisla State Hospital, Sivas, Turkey.

## Article Info

Received: 1 March 2024  
Accepted: 16 April 2024  
Available Online: 15 June 2024  
DOI: 10.3329/bjp.v19i2.71704

### Cite this article:

Yulak F, Keskin Z. A PLK1 inhibitor, RO3280, suppresses proliferation of SNU-16 gastric cancer cells via apoptosis. Bangladesh J Pharmacol. 2024; 19: 43-51.

## Abstract

This study examines the anti-tumor, pro-apoptotic, and genotoxic effects of polo-like kinase 1 (PLK1) inhibitor RO3280 on the gastric cancer cell line SNU-16. Using the XTT assay, the antiproliferative effect of the compound was identified and showed a significant antiproliferative effect ( $p < 0.01$ ) with the  $IC_{50}$  value of 9.64  $\mu$ M for 24 hours. RO3280 considerably enhanced the expression of Bax and cleaved caspase-3 ( $p < 0.01$ ) and dramatically lowered the BCL-2 level ( $p < 0.01$ ), demonstrating an apoptotic effect. It greatly raised the expression of 8-oxo-dG, a DNA damage marker, and cleaved PARP, a degraded version of the PARP enzyme involved in DNA repair ( $p < 0.05$  and  $p < 0.01$ , respectively). In addition, flow cytometric studies for annexin V and caspase-3/7 revealed that RO3280 markedly improved the apoptotic cell profile ( $p < 0.01$ ). It reduced the mitochondrial membrane potential and DNA damage ( $p < 0.01$ ). These findings suggest that RO3280 has an antitumor impact by damaging DNA and inducing apoptosis in SNU-16 gastric cancer cells.

## Introduction

Gastric cancer continues to be one of the most prevalent cancer forms diagnosed, despite a recent decline in frequency. In terms of the frequency of cancer-related mortality, it comes in third (Bray et al., 2018). Even though surgery is the primary treatment for early gastric cancer, most patients are diagnosed at an advanced stage and thus, chemotherapy has become the preferred course of action for these individuals (Kang et al., 2021). Nevertheless, chemotherapy has little influence on survival in individuals who are in advanced stages, and its adverse effects cause a lot of issues throughout treatment (Smyth et al., 2020). Even after resection, there is a chance of metastasis and recurrence of gastric cancer. Only 20 to 30 percent of patients survive within five years of surgery (Song et al., 2018), indicating that the prognosis is dismal. Individualized and targeted thera-

pies have emerged as an increasingly significant issue in the treatment of gastric cancer, replacing simpler surgical procedures with more intricate surgical procedures and chemotherapy (Bang et al., 2010).

Polo-like kinases are essential for mitosis, especially during the transition from G2 to cytokinesis (Archambault and Glover, 2009; Petronczki et al., 2008). Humans have been found to have five different subtypes of these kinases, each playing a unique part in the cell cycle (Bruinsma et al., 2012). In recent years, polo-like kinase 1 (PLK1)-related molecular interactions have drawn a lot of attention and have been thoroughly investigated. PLK1 is a crucial protein in the regulation of DNA damage and cell cycle progression (Takaki et al., 2008). PLK1 overexpression has been seen in a wide variety of tumor types, including those involving the gastric, prostate, breast, colorectal, lung, ovarian, testicular, and



hepatocellular malignancies (Eckerdt et al., 2005; Weichert et al., 2006) yet, PLK1 overexpression is hardly or only modestly detectable in normal tissues. Tumors with high levels of PLK1 expression frequently have a poor prognosis and low survival rates (Ng et al., 2016).

PLK1 has become a promising target as a result of the recent finding that inhibiting PLK1 expression causes tumor to induce antiproliferative effect, cell cycle arrest, and apoptosis. Consequently, some clinical trials have been carried out to develop new chemotherapeutics. There trials using various PLK1 inhibitors, including HMN-214, onvansertib, GSK 461364A, BI 6727, and BI 2536, have been carried out recently in a variety of cancer types (Ataseven et al., 2023; Chilamakuri et al., 2022; Gheghiani et al., 2020; Zeidan et al., 2020). The antitumor activity of RO3280 was assessed on MCF-7 human breast cancer cell lines, HepG2 human hepatocellular cancer cell lines, and PC3 human prostate cancer cell lines. In all cell lines, RO3280 exhibited a dose-dependent antitumor effect and caused apoptosis in MCF-7 cells (Ergul and Bakar-Ates, 2021).

The effectiveness of RO3280, a recently discovered potent and highly selective PLK1 inhibitor, has been investigated in many cancer types (Tao et al., 2017; Pajtler et al., 2017). The purpose of this study was to identify the pathways responsible for the antiproliferative activity of RO3280, a new PLK1 inhibitor, on the SNU-16 cell line generated from gastric cancer cells.

## Materials and Methods

### Cell line and cell culture

The American Type Culture Collection (ATCC), based in the USA, provided the SNU-16 cell line (CRL-5974)

for use. The cells used were acquired from Roswell Park Memorial Institute Medium (RPMI) where cells were cultured at 37°C in a 95% air and 5% CO<sub>2</sub> environment. Fetal bovine serum (FBS, 10%), L-glutamine (1%), and penicillin/streptomycin (1%) were present in RPMI-1640. DMSO was used to dissolve RO3280 (Sigma-Aldrich, UK), which was subsequently diluted with the medium. The concentration of DMSO was adjusted to be less than 0.1% before the chemical was administered to the cells. All of the ingredients used in the experiment, excluding the cell line, were obtained from Sigma-Aldrich, UK.

### Estimation of Bax, caspase 3, BCL-2, cleaved PARP, and 8-hydroxy-deoxyguanosine (8-oxo-dG) levels

The levels of Bax, cleaved caspase 3, BCL-2, cleaved PARP, and 8-oxo-dG in RO3280-treated and -untreated SNU-16 cells were measured using specific ELISA kits. For the corresponding assays, human ELISA kits from the BT Lab Shanghai, China, were utilized to assess Bax, cleaved caspase 3, BCL-2, cleaved PARP, and 8-oxo-dG. For ELISA testing, RO3280 was administered to SNU-16 cells in a 6-well plate at a dosage of 9.64 μM (IC<sub>50</sub>) for 24 hours (Ergul and Bakar-Ates, 2020). SNU-16 cells were taken from the RO3280-treated group and the control group after the treatment, PBS was added, and several freeze-thaw cycles were performed to cause cellular damage. SNU-16 cells from the RO3280-treated and control groups were taken after the treatment, PBS was added, and several freeze-thaw cycles were performed to cause cellular damage. The manufacturer's recommendations were followed for measuring the concentrations of these markers in the resulting cell lysates. Additionally, the BCA assay (Pierce Biotechnology, U.S.A) was used to measure the total protein concentrations of SNU-16 cells in the groups.

### Box 1: XTT assay

#### Principle

The XTT (sodium 3'-[1-(phenylaminocarbonyl)-3,4-tetrazolium]-bis(4-methoxy6-nitro)benzene sulfonic acid hydrate) assay is a colorimetric method to measure cellular metabolic activity as an indicator of cell viability, proliferation and cytotoxicity. This assay is based on the reduction of a yellow colored XTT to an orange formazan dye by metabolically active cells.

#### Requirements

Incubator (Nuve EC 160, Turkey); Microplate reader (Thermo Fisher Scientific, UK); RO3280; SNU-16 cell lines; XTT; 96-Well plate

#### Procedure

*Step 1:* In 96-well plates, the cells (1×10<sup>4</sup> cells/well) were seeded (50 μL/well).

*Step 2:* The cells were treated with different concentrations (1, 5, 10, 25, 50, and 100 μM) (50 μL/well) of RO3280 for 24 hours.

No treatment was applied to the cells in the control group.

*Step 3:* XTT (50 μL) was added to each well at a final volume of 150 μL after the initial incubation time and incubated for an additional 4 hours.

*Step 4:* Using a microplate reader, absorbances at 450 nm wavelengths were measured. All tests were repeated three times.

#### Calculation

The percentage of cell viability was calculated using the equation:

$$[\text{mean OD of treated cells} / \text{mean OD of control cells}] \times 100$$

GraphPad Prism was used to calculate the IC<sub>50</sub> value of the compound RO3280.

#### References

Joha et al., 2023

#### References (Video)

Filiz et al., 2021

### Annexin V binding assay

A total of  $5 \times 10^5$  SNU-16 cells were seeded in 6-well plates (Yulak et al., 2023), after which they were exposed to RO3280 at a concentration of  $9.64 \mu\text{M}$ , and they were then given another 24 hours of incubation. Cells were taken after the incubation time and resuspended in PBS containing at least 1% FBS. Following the manufacturer's directions, the cell suspension was then combined with an equivalent volume of annexin V and dead cell reagent. The millipore muse cell analyzer (Millipore, USA) was used to measure different cell populations, including live, dead, early, and late apoptotic cells.

### Evaluation of caspase 3/7 by flow cytometry

The muse caspase-3/7 kit was used to detect caspase 3/7. Initially, RO3280 was applied to SNU-16 cells ( $5 \times 10^5$ ) in a 6-well plate at a dosage of  $9.64 \mu\text{M}$ , and the cells were then incubated for 24 hours. Cells were collected the following day with a  $50 \mu\text{L}$  amount of cell solution in each tube. After that, the cells were incubated for 30 min at  $37^\circ\text{C}$  with  $5 \mu\text{L}$  of the caspase 3/7 working solution. The cells were then exposed to  $150 \mu\text{L}$  of 7-AAD (7-aminoactinomycin D) dye, which was left on the cells for 5 min at room temperature and in the dark. The muse cell analyzer was then used to detect cells.

### DNA damage assay

The muse multi-color DNA damage kit was used to measure ATM and H2AX activation by the instructions provided by the manufacturer (Ergul and Bakar-Ates, 2019). Briefly, cells were cultured at  $37^\circ\text{C}$  for 24 hours while being exposed to RO3280 at dose of  $9.64 \mu\text{M}$ . Cells were centrifuged after which they were washed once with PBS, fixed in fixation buffer, and washed in ice-cold buffer before being permeabilized. Each tube containing the cell suspension was then filled with  $10 \mu\text{L}$  of the antibody cocktail solution, and each was left to sit at room temperature in the dark for 30 min. Cells were resuspended in  $200 \mu\text{L}$  of 1x assay buffer after the final centrifugation and washing steps, and the percentages of negative cells (those with no DNA damage), ATM-activated cells, H2AX-activated cells, and DNA double-strand breaks were calculated using the muse cell analyzer.

### Evaluation of mitochondrial membrane potential by flow cytometry

The mitochondrial transmembrane potential was evaluated using the muse mitopotential kit. SNU-16 cells ( $5 \times 10^5$ ) were initially cultivated in a 6-well plate and treated with RO3280 at a dosage of  $9.64 \mu\text{M}$  for 24 hours. Cells were harvested the next day with  $100 \mu\text{L}$  of cell suspension in each tube. After that, cells were stained with muse™ MitoPotential dye and incubated for 20 min at  $37^\circ\text{C}$ . Cells were then exposed to  $5 \mu\text{L}$  of muse

mitopotential 7-AAD reagent for 5 min at room temperature and in the dark. Using the muse cell analyzer, percentages of viable, depolarized, depolarized/dead, and dead cells were calculated.

### Statistical analysis

The Kruskal-Wallis ANOVA test with post hoc Dunn or Mann-Whitney testing was used to examine the laboratory data, which were displayed as means with  $\pm$  standard deviations. For acceptance of statistically significant differences, a p-value of 0.01 was used. Data analysis and graphical presentations were done using the American program GraphPad Prism 7.0.

## Results

### Antiproliferative effect

The results of the XTT experiment showed that RO3280 significantly decreased the cell viability in a dose-dependent manner ( $p < 0.01$ ; Figure 1).

### Effect on Bax, BCL-2, cleaved caspase-3, cleaved PARP, and 8-oxo-dG proteins

RO3280 appeared to cause apoptosis because it caused a decrease in the anti-apoptotic protein BCL-2 and an increase in cleaved caspase-3 as a result of the breakdown of the apoptotic protein Bax. Additionally, during apoptosis, caspase-3 cleaves PARP, an enzyme involved in DNA damage and repair mechanisms, resulted in the production of cleaved PARP. After being exposed to RO3280, SNU-16 cells had higher amounts of cleaved PARP, which is evidence of its apoptotic action. Further, the observed rise in 8-oxo-dG levels following RO3280 treatment suggested that it promoted DNA damage in SNU-16 cells ( $p < 0.05$  to  $p < 0.01$ ; Table I).

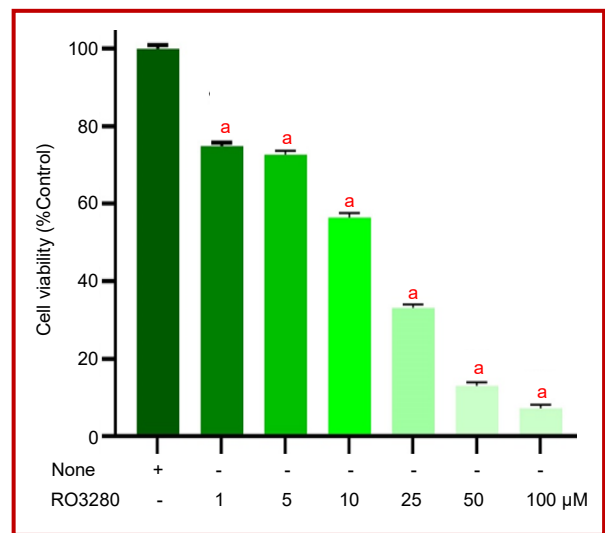


Figure 1: Antiproliferative effect of RO3280 on SNU-16 cell line

Table I					
Effects of RO3280 on Bax, BCL-2, cleaved caspase-3, cleaved PARP and 8-oxo-dG proteins					
	Bax (ng/mg protein)	BCL-2 (ng/mg protein)	Cleaved caspase-3 (ng/mg protein)	Cleaved PARP (ng/mg protein)	8-Oxo-dG (ng/mg protein)
Control	15.7 ± 1.4	59.4 ± 2.3	310.2 ± 30.1	850.3 ± 30.1	32.2 ± 2.1
RO3280-treated (9.64 µM)	22.5 ± 1.1 <sup>a</sup>	40.7 ± 2.9 <sup>a</sup>	850.5 ± 30.8 <sup>a</sup>	1098.4 ± 35.7 <sup>b</sup>	42.7 ± 2.5 <sup>a</sup>
When compared to control <sup>a</sup> p<0.01; <sup>b</sup> p<0.05					

### Apoptotic effect

When compared to the control group, it was found that RO3280-treated cells dramatically increased the rate of apoptosis. In RO3280-treated cells, the rates of late apoptosis and dead cells were determined to be 28.1% and 12.2%, respectively. These rates were significantly higher than in control cells (8.5%, 2.9%). From 85.4% to 58.4%, the proportion of viable cells drastically dropped. RO3280 considerably increased apoptosis in SNU-16 cells and contributed significantly to its antiproliferative effect ( $p < 0.01$ ; Figure 2A).

### Effect on caspase 3/7

The apoptotic/dead cell ratio in the control group was observed at 1.5%. These rates, however, significantly increased in the RO3280-treated group, and the apoptotic/dead cell ratio was calculated to be 22.8%. The dead cell ratio increased dramatically to 44% in the RO3280 group, from 7.3% in the control group. From 91% to 32.3%, the percentage of viable cells considerably dropped ( $p < 0.01$ ; Figure 2B). RO3280 markedly enhanced the number of caspase-3/7 in SNU-16 cells, which markedly promoted apoptosis.

### Effect on DNA damage

The results showed that RO3280 treatment significantly induced the phosphorylation levels of H2AX and ATM. The percentage of DNA double-strand breakage and single-strand breakage (pATM) in control cells (1.1%, 1%, respectively) increased to 3.6% and 6% in the RO3280-treated group, respectively ( $p < 0.05$  to  $p < 0.01$ ; Figure 2C).

### Effect on mitochondrial membrane potential

The depolarized/live cell ratio in the control group was 8.6%. However, there was a considerable rise, reaching 22.7% ( $p < 0.01$ ; Figure 2D), in the RO3280-treated group. Cells' apoptotic processes were triggered when the potential of the mitochondria was disrupted. Increased depolarization in the mitochondria of SNU-16 cells resulted in mitochondrial malfunction and the start of the cell's apoptotic processes. This approach also confirmed RO3280-induced apoptosis in SNU-16 cell lines.

## Discussion

In the present study, RO3280 demonstrated a signifi-

cant antiproliferative effect and significantly induced apoptosis, increased the expression of Bax, cleaved caspase-3, 8-oxo-dG, and cleaved PARP, and significantly decreased BCL-2 levels in subsequent experiments with the IC<sub>50</sub> dose. Additionally, flow cytometry studies using annexin V and caspase-3/7 demonstrated an increase in the number of apoptotic cells after medication treatment. Further, RO3280 reduced the mitochondrial membrane potential and impaired DNA in SNU-16 cells.

The primary regulating process of cell growth and proliferation is apoptosis, commonly referred to as programmed cell death. In response to particular induction signals, cells start intracellular processes resulting in recognizable physiological changes. These include externalization of phosphatidylserine to the cell surface, cleavage and degradation of particular cellular proteins, chromatin condensation and break-age, and disruption of membrane integrity (Kerr et al., 1972; Majno and Joris, 1995; Rudin and Thompson, 1997; Wyllie, 1993; Wyllie et al., 1980). Typically found on the inner surface of cell membranes, phosphatidylserine is a membrane component that is bound by the calcium-dependent phospholipid-binding protein known as annexin V (Andree et al., 1990; Tait et al., 1989; van Heerde et al., 1995). Early in the process of apoptosis, PS molecules migrate to the cell membrane's periphery and are readily able to bind to annexin V.

In response to proapoptotic signals, cysteine proteases called caspases play a crucial part in the continuation of the process of programmed cell death (apoptosis) (Riedl and Shi, 2004). When a cell experiences an apoptotic stimulus, they are produced in cells as zymogens and are cleaved to their active substrates, causing apoptosis (Bakar-Ates et al., 2020). Some caspases, known as initiator caspases, function to start the intracellular apoptotic process, whereas effector caspases, such as caspases 3 and 7, have a direct impact on cellular lysis by cleaving structural proteins. The most prominent of the caspases, caspase 3, activates the endonuclease CAD (caspase-activated DNase), which results in chromatin condensation and chromosomal DNA degradation (Jan and Chaudhry, 2019). Apoptosis is thus characterized by caspase-3/7 activation (Porter and Janicke, 1999). Additionally, the protein PARP plays a crucial role in DNA repair pathways, particularly in the repair of base

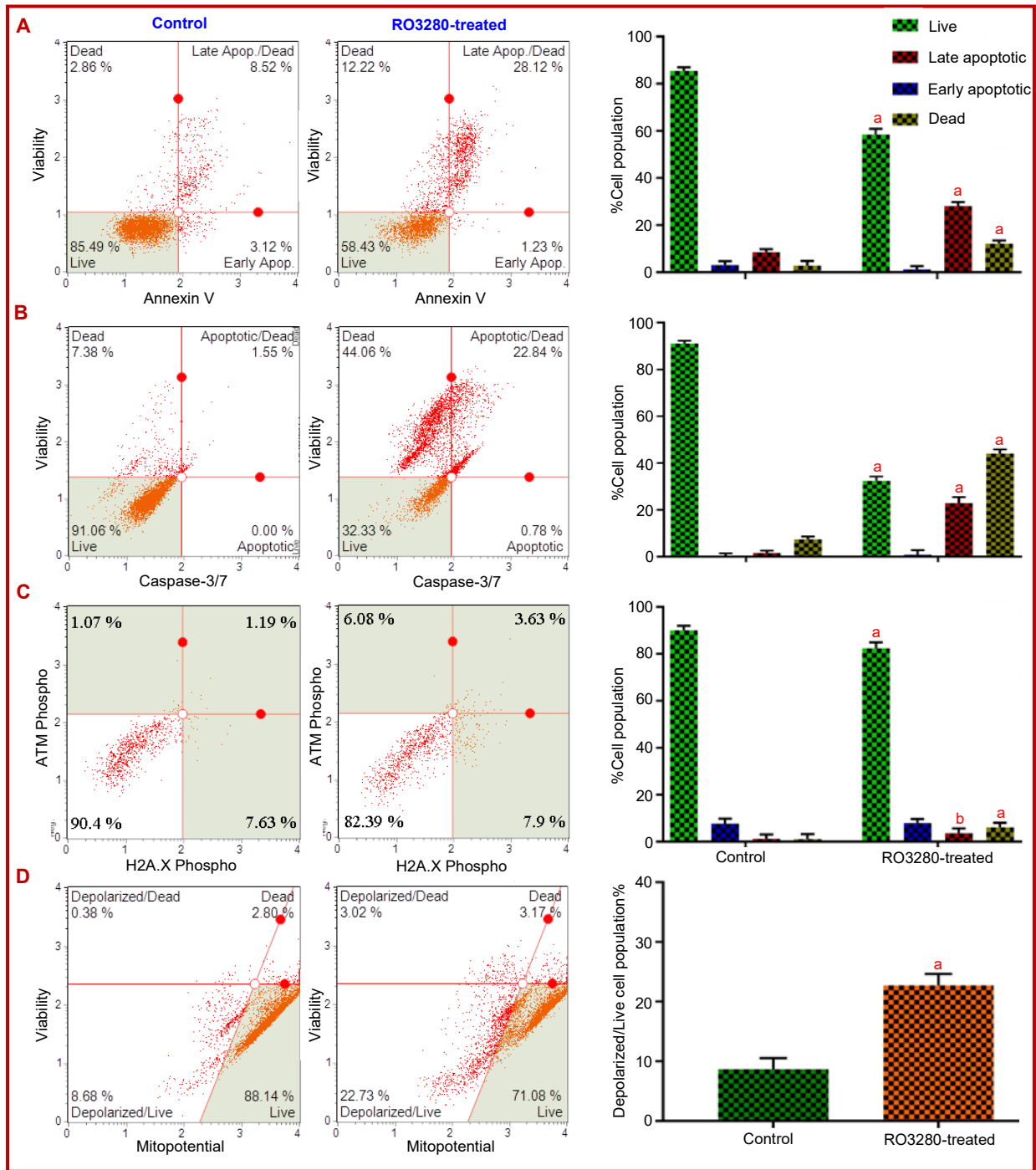


Figure 2: Effects RO3280 (9.64  $\mu$ M) annexin V (A), caspase 3/7 (B), H2A.X phospho (C) and mitopotential (D) in SNU-16 cell lines

excisions, and its cleavage or inhibition kills cells by taking advantage of a flaw in DNA repair (Sachdev et al., 2019). This protein is also one of the substrates of active caspases that has received the most research (Tang et al., 2018).

The pro-apoptotic protein Bax causes the mitochondrial membrane to rupture during the apoptotic process, releasing cytochrome c and creating the so-called apoptosome. This complex includes the proteins cytochrome

c, caspase-9, and Apaf-1, which activate effector caspases and cause apoptosis (Carneiro and El-Deiry, 2020). BCL-2, on the other hand, prevents the release of cytochrome c and suppresses apoptosis (Baig vd., 2016). Effectively connected to the mechanism of cell death are increased pro-apoptotic Bax and decreased BCL-2. A cell's destiny is frequently determined by the ratio of pro- and anti-apoptotic proteins, such as Bax and BCL-2 (Cavalcante et al., 2019; Wong, 2011).

The major goal of cancer therapy is to induce apoptotic cell death, one of the defenses against the onset and spread of cancer (Tang et al., 2018). In order to determine if the antiproliferative impact of RO3280 is linked to DNA damage, was also used an 8-oxo-dG ELISA to assess DNA fragmentation in SNU-16 cells after 24 hours of RO3280 treatment. A well-known indicator of DNA oxidative damage is 8-oxo-dG (Guo et al., 2020). The results demonstrated that treatment with RO3280 dramatically increased the levels of 8-oxo-dG in SNU-16 cells, supporting its antiproliferative and apoptotic actions. By using flow cytometry and ELISA tests, the current study confirmed that RO3280 causes DNA damage. Anti-apoptotic BCL-2 protein levels are markedly reduced by RO3280 therapy, whereas pro-apoptotic Bax and cleaved caspase 3 levels are up-regulated and cleaved PARP levels are increased. These findings demonstrated unequivocally that RO3280 caused DNA damage and caused apoptosis in SNU-16 cells.

The energy balance of the cell is maintained by mitochondria, which also contain important regulators of cell death processes including apoptosis. Therefore, mitochondrial alterations are a crucial sign of a healthy cell. In these healthy cells, the energy accumulated during mitochondrial respiration forms a mitochondrial transmembrane potential that allows the cell to control the synthesis of ATP. The energy accumulated during mitochondrial respiration is stored as an electrochemical gradient across the mitochondrial membrane. The early phases of apoptosis have been found to typically be correlated with the loss of the mitochondrial internal transmembrane potential (Finkel, 2001; Hearps et al., 2002; Krysko et al., 2001; Ly et al., 2003; X. Wang, 2001; Zamzami and Kroemer, 2001; Zamzami et al., 1996). The opening of mitochondrial permeability transition pores, which results in the release of cytochrome C into the cytosol and ultimately starts the apoptotic cascade, are thought to occur simultaneously with the collapse of this potential. Changes in the mitochondrial membrane potential have been connected to caspase-independent cell death, necrotic cell death, and apoptosis. In the study of apoptosis, drug toxicity, and various disease states, depolarization of the inner mitochondrial membrane potential is a valid sign of mitochondrial malfunction and cellular health. Apoptosis is triggered by damage to the mitochondrial membrane (Lee et al., 2019). RO3280 promotes apoptosis through the mitochondrial pathway, according to ~~our~~ this research on mitochondrial membrane potential.

Numerous tumor types have been demonstrated to exhibit PLK1 overexpression. PLK1 inhibitors are being researched and developed in relation to this for the treatment of cancer (Otto and Sicinski, 2017). The literature has numerous studies that support the results. The impact of PLK1 inhibition on breast cancer cells was examined in a recent study. PLK1 inhibitor BI-2536 demonstrated antiproliferative effects and promoted

apoptosis in breast cancer cells (Ueda et al., 2019).

PLK1 was discovered to be substantially expressed in leukemia cells in pediatric acute myeloid leukemia lines in another study. On primary ALL and AML cells, RO3280 had an antiproliferative impact and caused apoptosis. Additionally, RO3280 administration increased the expression of genes linked to apoptosis, including DCC, CDKN1A, BTK, and SOCS2; this overexpression was verified by western blotting (Wang et al., 2015).

Another recent study examined the effects of RO3280 on bladder cancer *in vivo* and *in vitro*. RO3280 enhanced wee1 expression and cell cycle protein 2 phosphorylation while decreasing cell proliferation and cell cycle progression. Additionally, it enhanced cleaved PARP and caspase-3 and caused apoptosis. Additionally, BubR1 expression was reduced. The *in vivo* portion of the study showed that RO3280 inhibited the growth of a bladder cancer xenograft in a mouse model (Zhang et al., 2017). In this study, RO3280 enhanced cleaved PARP and caspase-3, decreased cell proliferation, and triggered apoptosis.

Another investigation examined the *in vivo* and *in vitro* antitumoral effects of the PLK1 inhibitor GSK461364 on neuroblastoma cells. In neuroblastoma cells, treatment with GSK461364 reduced cell viability and proliferative potential. It also caused apoptosis and halted the cell cycle. In mice, therapy with GSK461364 considerably slowed the growth of xenograft tumors *in vivo* and boosted survival rates. According to these preclinical results, PLK1 inhibitors might be useful for high-risk or relapsed individuals (Pajtler et al., 2017).

Another study investigated how pancreatic cancer cells responded to the PLK1 inhibitor GSK461364A. The cell cycle was interrupted and the rate of DNA synthesis was markedly lowered when PLK1 was inhibited. Additionally, it was evaluated GSK461364A's impact in conjunction with gemcitabine and found that PLK1 inhibition dramatically enhanced gemcitabine's anticancer effects in both *vivo* and *vitro*. It was drawn the conclusion that PLK1 inhibition can be employed to treat malignancies that are resistant to conventional chemotherapies or to increase chemotherapy effectiveness (Li et al., 2016).

A PLK1 inhibitor, GSK461364A, was administered to five cell lines, Raji, K562, PC3, MCF-7, MDA-MB-231, and noncancerous L929 cell line, and its antiproliferative effect was assessed by XTT assay in a study. In all cancer groups, GSK461364A demonstrated a strong antiproliferative effect. The antiproliferative effect of non-cancerous cells was found to be low. The DNA damage response was considerably changed after GSK-461364A treatment in Raji cells. GSK461364A therapy significantly increased the percentage of early and late apoptotic cells, in compliance with an annexin V

binding assay. Additionally, GSK461364A therapy dramatically caused Raji cell death, as demonstrated by fluorescence imaging. Increased expression of Bax and cleaved caspase 3 as well as decreased expression of BCL-2 further supported the apoptotic impact (Ergul and Bakar-ates, 2020).

PLK1 inhibitors boosted the efficacy of cisplatin, decreased proliferation, and increased apoptosis rates in the drug-treated cell line, in accordance with a study on the effects of PLK1 inhibitor BI2536 and si-PLK1 on cisplatin-resistant gastric cancer cells. Additionally, cyclin B1 and CDC25C, two molecules that control cell division, were at reduced levels. This data suggests that cisplatin resistance in gastric cancer cells may result from PLK1 overexpression, and that PLK1 inhibition may be used to decrease resistance and improve treatment effectiveness (Chen et al., 2019).

It was discovered that PLK1 depletion decreased polydifferentiation and procaspase 3 levels and promoted apoptosis in gastric cancer cells in another study that examined the impact of PLK1 inhibition on gastric cancer cells (Chen et al., 2006). Similar to these investigations, this study also found that PLK1 inhibition led to apoptosis by exerting antiproliferative effects on gastric cancer cells and exhibiting anticancer efficacy.

The study has limitations such as the apoptotic effect caused by RO3280 in SNU-16 cells need to be supported by different methods such as calcium flux and western blot analysis.

---

## Conclusion

A PLK1 inhibitor, RO3280, has shown a substantial antitumor effect on the SNU-16 gastric cancer cell line and is a candidate to be used as an alternative therapy for the treatment of gastric cancer.

---

## Financial Support

Self-funded

---

## Ethical Issue

Cell lines derived from expansion of primary cell cultures *in vitro* are not relevant material, as all of the original cells will have divided and so the cell line has been created outside of the human body. The storage and use of cell lines created from primary human tissue, for research purposes, does not require an ethical approval.

---

## Conflict of Interest

Authors declare no conflict of interest

---

## References

- Andree HAM, Reutlingsperger CPM, Hauptmann R, Hemker HC, Hermens WT, Willems GM. Binding of vascular anti-coagulant  $\alpha$  (VAC $\alpha$ ) to planar phospholipid bilayers. *J Biol Chem.* 1990; 265: 4923-28.
- Archambault V, Glover DM. Polo-like kinases: Conservation and divergence in their functions and regulation. *Nat Rev Mol Cell Biol.* 2009; 10: 265-75.
- Ataseven D, Tastemur S, Yulak F, Karabulut S, Ergul M. GSK461364A suppresses proliferation of gastric cancer cells and induces apoptosis. *Toxicol in Vitro.* 2023; 90: 105610.
- Baig S, Seevasant I, Mohamad J, Mukheem A, Huri HZ, Kamarul T. Potential of apoptotic pathway-targeted cancer therapeutic research: Where do we stand? *Cell Death Dis.* 2016; 7: e2058.
- Bakar-Ates F, Ozkan E, Sengel-Turk CT. Encapsulation of cucurbitacin B into lipid polymer hybrid nanocarriers induced apoptosis of MDAMB231 cells through PARP cleavage. *Intern J Pharm.* 2020; 586: 119565.
- Bang YJ, Van Cutsem E, Feyereislova A, Chung HC, ShenL, Sawaki A, Kang YK. Trastuzumab in combination with chemotherapy versus chemotherapy alone for treatment of HER2-positive advanced gastric or gastro-oesophageal junction cancer (ToGA): A phase 3, open-label, randomised controlled trial. *Lancet* 2010; 376: 687-97.
- Bray F, Ferlay J, Soerjomataram I, Siegel RL, TorreLA, Jemal A. Global cancer statistics 2018: GLOBOCAN estimates of incidence and mortality worldwide for 36 cancers in 185 countries. *CA Canc J Clinic.* 2018; 68: 394-424.
- BruinsmaW, Raaijmakers JA, Medema RH. Switching polo-like kinase-1 on and off in time and space. *Trends Biochem Sci.* 2012; 37: 534-42.
- Carneiro BA, El-Deiry WS. Targeting apoptosis in cancer therapy. *Nat Rev Clin Oncol.* 2020; 17: 395-417.
- Cavalcante GC, Schaan AP, Cabral GF, Santana-Da-Silva MN, Pinto P, Vidal AF, Ribeiro-Dos-Santos A. A cell's fate: An overview of the molecular biology and genetics of apoptosis. *Int J Mol Sci.* 2019; 20: 1-20.
- Chen XH, Lan B, Qu Y, Zhang XQ, Cai Q, Liu BY, Zhu ZG. Inhibitory effect of polo-like kinase 1 depletion on mitosis and apoptosis of gastric cancer cells. *World J Gastroenterol.* 2006; 12: 29-35.
- Chen Z, ChaiY, Zhao T, Li P, Zhao L, He F, Ju H. Effect of PLK1 inhibition on cisplatin-resistant gastric cancer cells. *J Cell Physiol.* 2019; 234: 5904-14.
- Chilamakuri R, Rouse DC, Agarwal S. Inhibition of polo-like kinase 1 by HMN-214 blocks cell cycle progression and inhibits neuroblastoma growth. *Pharmaceuticals (Basel)* 2022; 15: 523.
- Eckerdt F, Yuan J, Strebhardt K. Polo-like kinases and oncogenesis. *Oncogene* 2005; 24: 267-76.
- Ergul M, Bakar-Ates F. A specific inhibitor of polo-like kinase 1, GSK461364A, suppresses proliferation of Raji Burkitt's lymphoma cells through mediating cell cycle arrest, DNA damage, and apoptosis. *Chem-Biol Interact.* 2020; 332:



- 109288.
- Ergul M, Bakar-Ates F. RO3280: A novel PLK1 inhibitor, suppressed the proliferation of MCF-7 breast cancer cells through the induction of cell cycle arrest at G2/M point. *Anticancer Agents Med Chem.* 2019; 19: 1846-54.
- Ergul M, Bakar-Ates F. Investigation of molecular mechanisms underlying the antiproliferative effects of colchicine against PC3 prostate cancer cells. *Toxicol in Vitro.* 2021; 73: 105138.
- Filiz AK, Joha Z, Yulak F. Mechanism of anti-cancer effect of  $\beta$ -glucan on SH-SY5Y cell line. *Bangladesh J Pharmacol.* 2021; 16: 122-28.
- Finkel E. The mitochondrion: Is it central to apoptosis? *Science* 2001; 292: 624-26.
- Gheghiani L, Shang S, Fu Z. Targeting the PLK1-FOXO1 pathway as a novel therapeutic approach for treating advanced prostate cancer. *Sci Rep.* 2020; 10: 12327.
- Guo Q, Zhang H, Deng Y, Zhai S, Jiang Z, Zhu D, Wang L. Ligand- and structural-based discovery of potential small molecules that target the colchicine site of tubulin for cancer treatment. *Eur J Med Chem.* 2020; 196: 112328.
- Hearps AC, Burrows J, Connor CE, Woods GM, Lowenthal RM, Ragg SJ. Mitochondrial cytochrome c release precedes transmembrane depolarisation and caspase-3 activation during ceramide-induced apoptosis of Jurkat T cells. *Apoptosis* 2002; 7: 387-94.
- Jan R, Chaudhry GS. Understanding apoptosis and apoptotic pathways targeted cancer therapeutics. *Adv Pharm Bull.* 2019; 9: 205-18.
- Joha, Z, Ozturk A., Yulak F, Karatas O, Ataseven H. Mechanism of anticancer effect of gambogic acid on gastric signet ring cell carcinoma. *Med Oncol.* 2023; 40: 1-8.
- Kang YK, Yook JH, Park YK, Lee JS, Kim YW, Kim JY, Noh SH. PRODIGY: A phase III study of neoadjuvant docetaxel, oxaliplatin, and S-1 plus surgery and adjuvant s-1 versus surgery and adjuvant s-1 for resectable advanced gastric cancer. *J Clin Oncol.* 2021; 39: 2903-13.
- Kerr JF, Wyllie AH, Curri AR. Apoptosis: A basic biological phenomenon with wide-ranging implications in tissue kinetics. *Br J Cancer.* 1972; 26: 239-57.
- Krysko DV, Roels F, Leybaert L, D'Herde K. Mitochondrial transmembrane potential changes support the concept of mitochondrial heterogeneity during apoptosis. *J Histochem Cytochem.* 2001; 49: 1277-84.
- Lee S, Jeong YJ, Yu A, Kwak HJ, Cha J, Kang I. Carfilzomib enhances cisplatin-induced apoptosis in SK-N- BE (2)-M17 human neuroblastoma cells. *Sci Rep.* 2019; 9: 1-14.
- Li J, Wang R, Schweickert PG, Karki A, Yang Y, Kong Y, Liu X. Plk1 inhibition enhances the efficacy of gemcitabine in human pancreatic cancer. *Cell Cycle.* 2016; 15: 711-19.
- Ly JD, Grubb DR, Lawen A. The mitochondrial membrane potential ( $\Delta\psi(m)$ ) in apoptosis: An update. *Apoptosis* 2003; 8: 115-28.
- Majno G, Joris I. Apoptosis, oncosis, and necrosis. An overview of cell death. *Am J Pathol.* 1995; 146: 3-15.
- Ng WTW, Shin JS, Roberts TL, Wang B, Lee CS. Molecular interactions of polo-like kinase 1 in human cancers. *J Clin Pathol.* 2016; 69: 557-62.
- Otto T, Sicinski P. Cell cycle proteins as promising targets in cancer therapy. *Nat Rev Cancer.* 2017; 17: 93-115.
- Pajtlér KW, Sadowski N, Ackermann S, Althoff K, Schönbeck K, Batzke K, Schulte JH. The GSK461364 PLK1 inhibitor exhibits strong antitumoral activity in preclinical neuroblastoma models. *Oncotarget* 2017; 8: 6730-41.
- Petronczki M, Lenart P, Peters JM. Polo on the rise—from mitotic entry to cytokinesis with Plk1. *Dev Cell.* 2008; 14: 646-59.
- Porter AG, Jänicke RU. Emerging roles of caspase-3 in apoptosis. *Cell Death Differ.* 1999; 6: 99-104.
- Riedl SJ, Shi Y. Molecular mechanisms of caspase regulation during apoptosis. *Nat Rev Mol Cell Biol.* 2004; 5: 897-907.
- Rudin CM, Thompson CB. Apoptosis and disease: Regulation and clinical relevance of programmed cell death. *Annu Rev Med.* 1997; 48: 267-81.
- Sachdev E, Tabatabai R, Roy V, Rimel BJ, Mita MM. PARP inhibition in cancer: An update on clinical development. *Targ Oncol.* 2019; 14: 657-79.
- Smyth EC, Nilsson M, Grabsch HI, van Grieken NC, Lordick F. Gastric cancer. *Lancet* 2020; 396: 635-48.
- Song R, Hou G, Yang J, Yuan J, Wang C, Chai T, Liu Z. Effects of PLK1 on proliferation, invasion and metastasis of gastric cancer cells through epithelial-mesenchymal transition. *Oncol Lett.* 2018; 16: 5739-44.
- Tait JF, Gibson D, Fujikawa K. Phospholipid binding properties of human placental anticoagulant protein-I, a member of the lipocortin family. *J Biol Chem.* 1989; 264: 7944-49.
- Takaki T, Trenz K, Costanzo V, Petronczki M. Polo-like kinase 1 reaches beyond mitosis: Cytokinesis, DNA damage response, and development. *Curr Opin Cell Biol.* 2008; 20: 650-60.
- Tang H, Zhang Y, Li D, Fu S, Tang M, Wan L, Chen L. Discovery and synthesis of novel magnolol derivatives with potent anti-cancer activity in non-small cell lung cancer. *Eur J Med Chem.* 2018; 156: 190-205.
- Tao YF, Li ZH, Du WW, Xu LX, Ren JL, Li XL, Pan J. Inhibiting PLK1 induces autophagy of acute myeloid leukemia cells via mammalian target of rapamycin pathway dephosphorylation. *Oncol Rep.* 2017; 37: 1419-29.
- Ueda A, Oikawa K, Fujita K, Ishikawa A, Sato E, Ishikawa T, Kanekura K. Therapeutic potential of PLK1 inhibition in triple-negative breast cancer. *Lab Invest.* 2019; 99: 1275-86.
- van Heerde WL., de Groot PG, Reutelingsperger CP. The complexity of the phospholipid binding protein annexin V. *Thromb Haemost.* 1995; 73: 172-79.
- Wang NN, Li ZH, Zhao H, Tao YF, Xu LX, Lu J, Pan J. Molecular targeting of the oncoprotein PLK1 in pediatric acute myeloid leukemia: RO3280, a novel PLK1 inhibitor, induces apoptosis in leukemia cells. *Int J Mol Sci.* 2015; 16: 1266-92.
- Wang X. The expanding role of mitochondria in apoptosis. *Genes Dev.* 2001; 15: 2922-33.
- Weichert W, Ullrich A, Schmidt M, Gekeler V, Noske A, Nies-

- porek S, Denkert C. Expression patterns of polo-like kinase 1 in human gastric cancer. *Cancer Sci.* 2006; 97: 271-76.
- Wong RSY. Apoptosis in cancer: From pathogenesis to treatment. *J Exp Clin Cancer Res.* 2011; 30: 1-14.
- Wyllie AH. Apoptosis. *Br J Cancer.* 1993; 67: 205-08.
- Wyllie AH, Kerr JF, Currie AR. Cell death: The significance of apoptosis. *Int Rev Cytol.* 1980; 68: 251-306.
- Yulak F, Filiz AK, Joha Z, Ergul M. Mechanism of anticancer effect of ETP-45658, a PI3K/AKT/mTOR pathway inhibitor on HT-29 cells. *Med Oncol.* 2023; 40: 1-14.
- Zamzami N, Kroemer G. The mitochondrion in apoptosis: How Pandora's box opens. *Nat Rev Mol Cell Biol.* 2001; 2: 67-71.
- Zamzami N, Susin SA, Marchetti P, Hirsch T, Gomez-Monterrey I, Castedo M, Kroemer G. Mitochondrial control of nuclear apoptosis. *J Exp Med.* 1996; 183: 1533-44.
- Zeidan AM, Ridinger M, Lin TL, Becker PS, Schiller GJ, Patel PA, Wang ES. A phase Ib study of onvansertib, a novel oral PLK1 inhibitor, in combination therapy for patients with relapsed or refractory acute myeloid leukemia. *Clin Cancer Res.* 2020; 26: 6132-40.
- Zhang Z, Zhang G, Kong C. Targeted inhibition of polo-like kinase 1 by a novel small-molecule inhibitor induces mitotic catastrophe and apoptosis in human bladder cancer cells. *J Cell Mol Med.* 2017; 21: 758-67.
- 

**Author Info**

Fatih Yulak (Principal contact)  
e-mail: fatihyulak@gmail.com.tr